Kalman filter-based tracking of abdominal organ motions along the medial axis

Harini Veeraraghavan, Robert J. Jones, Daekun You, Neelam Tyagi, James M. Balter

Purpose/Objective: Modeling motion of organs along their natural axes as opposed to their sampled locations in Cartesian space allows for deeper understanding of motion sparsity, with potential advantages for rapid dynamic motion monitoring, dose response assessment, and generation of virtual twins to mimic human treatments. This investigation models and predicts the motion along the medial axis of abdominal organs due to breathing, stomach contractions, and slow drift of abdominal organs using a Kalman filter based approach.

Materials/Methods: A hierarchical model of abdominal motion [1] extracted from a golden angle stack of stars scan provided 21 canonical states of breathing (based on liver position), antral contraction (based on phase angle) and 72 slow drift (based on time) motion, as well as their combined deformation effects throughout the scan. The stomach, duodenum, colon, and small bowel were delineated on the breathing motion-corrected exhale reference state of this model, from which medial axis transforms were computed [2]. Deformation vector fields corresponding to the individual motion patterns were then applied to the medial axes to generate the temporal motion patterns for each organ. A linear Kalman filter modeling the displacement of the individual points within the medial axis for each organ modeled the motion of each point independently as a simple linear dynamic system in the three directions using displacement (observed) and uniform velocity (unobserved). The Kalman filter state thus consisted of 6 x N variables, N being the number of points along the medial axis. The Kalman filter was initialized with a state process covariance (P = 1000) and measurement error (R = 0.5) and subjected to Gaussian process noise of 1e-2. Errors in predicted displacements and estimated displacements were computed.

Results: The Kalman filter successfully estimated medial axis displacement with uncertainty decreasing progressively for the various motions. Errors in the predicted medial axis motion were highest for breathing induced motion for all organs (Table I). Breathing motion resulted in the largest displacement in the cranial-caudal direction for all organs with 10.57 +/- 11.43mm for the stomach followed by the duodenum at 7.11 +/- 7.64mm. On the other hand, the colon had the highest medial axis displacement in the anterior-posterior direction due to breathing (4.29 +/- 1.52mm) followed by the small bowel (3.13 +/- 3.35mm). In the lateral direction, slow drift resulted in the largest displacement for the colon (2.19 +/- 0.61mm) followed by the duodenum. Finally, antral contraction resulted in the largest displacement for the stomach in the lateral direction (1.07 +/- 1.19mm) followed by the colon (0.27 +/- 0.08mm) (Figure 1). Figure 2 shows Kalman filter predictions (gray squares) and the estimated motion of the medial axis at distinct canonical phases (t = 0, t=10, t=20) from the different motion patterns for the analyzed organs.

Conclusions: Kalman filtering was able to estimate the influence of different motion sources on organ deformations along the medial axis of the gastrointestinal tract and showed the ability to track organ motions under various conditions. The estimated errors were the highest due to breathing motion and occurred for the stomach as well as due to slow drift for the colon. Our results indicated that the largest displacements in the z-direction occurred from breathing, and the largest displacements in the x-direction occurred from slow drift. Our preliminary analysis shows feasibility to track the temporal trajectory of entire organs.

Table 1: Prediction errors of the Kalman filter-estimated canonical motion along medial axes.

Prediction error	Antral contraction			Breathing			Slow drift		
	X mm	Y mm	Z mm	X mm	Y mm	Z mm	X mm	Y mm	Z mm
Colon	1.04 ± 0.06	0.59 ± 0.02	1.04 ± 0.04	0.95 ± 0.35	2.87 ± 0.42	5.43 ± 1.56	1.34 ± 0.22	1.67 ± 0.53	1.52 ± 0.12
Stomach	1.09 ± 0.26	0.95 ± 0.07	0.76 ± 0.16	1.08 ± 0.17	2.20 ± 0.32	6.18 ± 1.28	0.59 ± 0.20	1.20 ± 0.19	0.63 ± 0.27
Duodenum	0.39 ± 0.07	0.46 ± 0.06	1.09 ± 0.07	0.71 ± 0.21	1.79 ± 0.35	5.21 ± 0.99	0.94 ± 0.31	1.02 ± 0.36	1.11 ± 0.25
Small bowel	1.01 ± 0.03	0.56 ± 0.02	1.33 ± 0.05	1.48 ± 0.27	2.47 ± 0.52	4.31 ± 0.66	1.22 ± 0.17	1.41 ± 0.33	1.61 ± 0.36

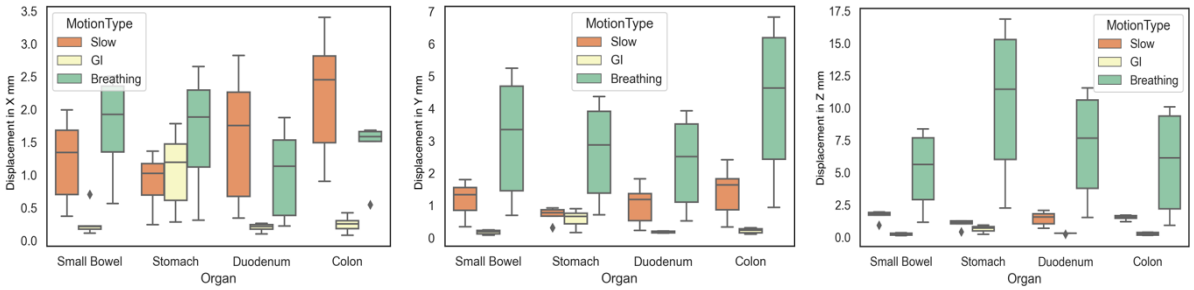

A. Displacement in X B. Displacement in Y C. Displacement in Z

Figure 1: Displacement of the medial axis for the various organs due to the analyzed motion as estimated using the Kalman filter.

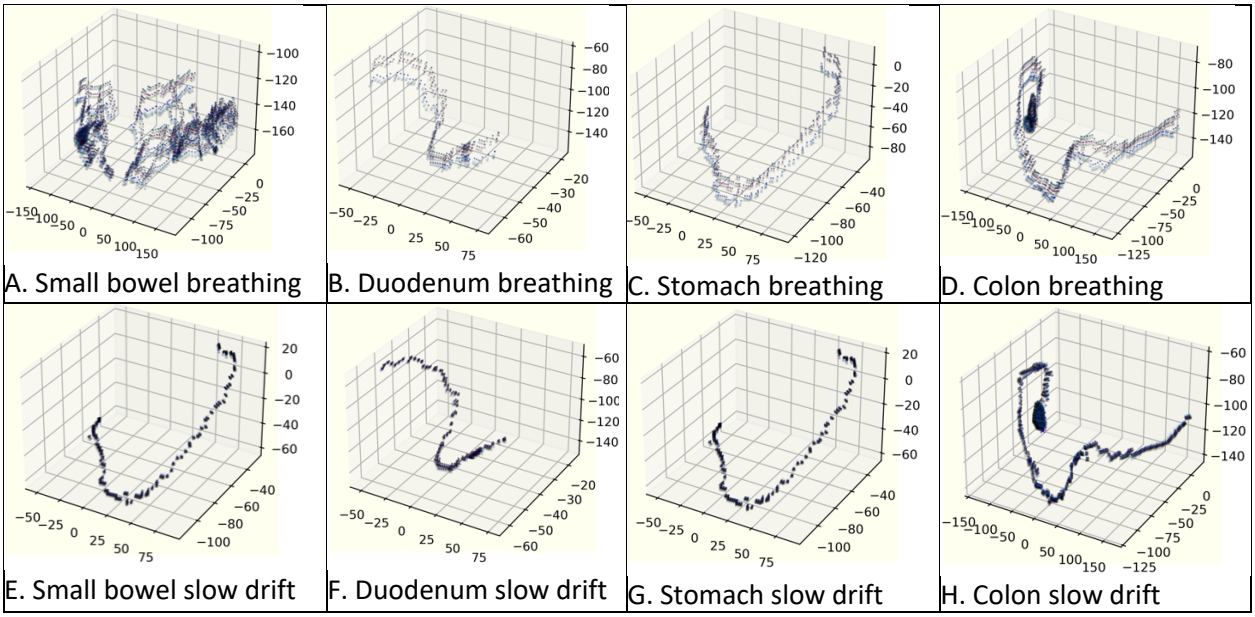

A. Small bowel breathing B. Duodenum breathing C. Stomach breathing D. Colon breathing

E. Small bowel slow drift F. Duodenum slow drift G. Stomach slow drift H. Colon slow drift

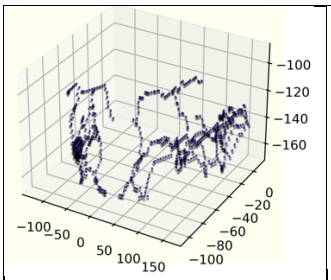

I. Small bowel antral contractions

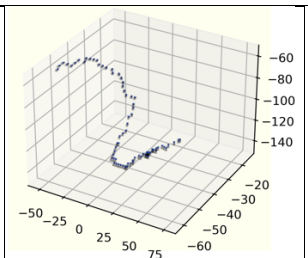

J. Duodenum antral contractions

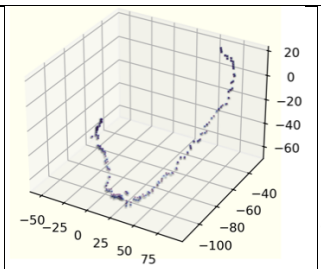

K. Stomach antral contractions

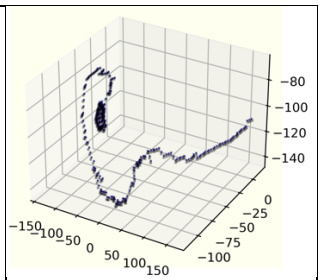

L. Colon antral contractions

Figure 2. Estimated medial axis displacements of various organs due to the different motion patterns.

1. Zhang, Y., et al., A hierarchical model of abdominal configuration changes extracted from golden angle radial magnetic resonance imaging. Phys Med Biol, 2021 Feb 9;66(4):045018
2. Ta-Chih Lee et.al., "Building skeleton models via 3-D medial surface/axis thinning algorithms." Computer Vision, Graphics, and Image Processing, 56(6):462–478, 1994